Electronic Supplementary Material (ESI) for Materials Chemistry Frontiers.

Supporting Information

Biomass-Derived Nitrogen and Sulfur Co-Doped Carbon Microtubes for Oxygen Reduction Reaction

Luting Song,[1] *Jinquan Chang,*[1] *Yanhong Ma,*[1] *Wenyu Jiang,*[1] *Yuanqing Xu,*[1] *Cheng Liang,*[1] *Zhexue Chen,*[1] *and Yong Zhang*[1,2]*

[1]CAS Key Laboratory of Nanosystem and Hierarchical Fabrication, CAS Center for Excellence in Nanoscience, National Center for Nanoscience and Technology, Beijing 100190, P. R. China

[2]University of Chinese Academy of Sciences, Beijing 100049, P. R. China

*Correspondence should be addressed to Yong Zhang (E-mail: zhangyong@nanoctr.cn)

Experimental section

The catkins were collected in the field by hand in Beijing, China. All the chemicals were analytical grade and commercially available from Aladdin Industrial Corporation and were used without further purification.

Preparation of the MB/catkin hybrids. The catkins were collected randomly, and washed by double distilled water and absolute ethanol for several times to get rid of the seeds and dusts. The white, cotton-like, mechanical-resilience catkins were then immersed in 1 g/L methylene blue (MB) solution overnight to make catkins adsorb MB molecules until saturation. The catkins saturated with MB molecules were dried at 90 ^{o}C in an oven for 24 h, resulting in the dark blue MB/catkin hybrids.

Preparation of the conductive N, S-CMTs. The as-prepared MB/catkin hybrids were transferred into a tube furnace for carbonization under flowing inert (Ar) atmosphere. The hybrids were heated directly to high temperature at the range from 700 to 900 ^{o}C for 2 h with a heating rate of 5 ^{o}C/min to generate the black N, S-CMTs. The carbonized samples with catkin-like morphology remained certain mechanical resilience, although it was lower than that of the pristine catkins.

Fabrication of the activated N, S-CMTs (CO_2) electrocatalysts. The as-prepared black N, S-CMTs were further activated in the tube furnace under flowing 2.5% CO_2/Ar atmosphere with a heating rate of 5 ^{o}C/min to 800 ^{o}C for 0.5, 1.5, and 2 h. The longer activation time resulted in more weight loss of the samples (weight loss ca. 30, 60, and 90%, respectively), which were named as N, S-CMT-800-30, N, S-CMT-800-60, and N, S-CMT-800-90.

Characterization. Scanning electron microscopy (SEM) and energy filtered scanning electron microscopy (EFSEM) were performed on a Hitachi SU8200 microscope operated at an acceleration voltage of 5 kV. High-resolution Transmission electron microscopy (HRTEM) and selected-area electron diffraction (SAED) pattern were acquired on a Tecnai G2 F20 U-TWIN microscope operated at an accelerating voltage of 200 kV. N_2 sorption measurements were conducted using a Micromeritics ASAP 2420 accelerated surface area and porosimetry system, at 77 K using Brunauer-Emmett-Teller (BET) calculations for the surface area. The pore size distribution (PSD) plots were acquired from the adsorption branch of the isotherm based on the

Barrett-Joyner-Halenda (BJH) model. X-ray photoelectron spectroscopy (XPS) was performed on a Thermo Scientific ESCALab 250Xi spectrometer with 300 W monochromatic Al Kα radiation. Raman spectroscopy was performed on a Renishaw inVia plus spectrometer with 532 nm laser to demonstrate the presence of the graphitic and amorphous carbon in the samples. Fourier transform infrared (FTIR) spectra were recorded on a PerkinElmer Spectrum One spectrometer with a scan range from 4000 to 500 cm^{-1} at room temperature.

Electrochemical measurements. The electrochemical measurements were carried out in a conventional three-electrode cell using an electrochemical workstation (VersaSTAT 3 Potentiostat/Galvanostat, Princeton Applied Research) operated at room temperature. A 4.0-mm diameter glassy carbon disk (disk geometric area 0.1256 cm^2) was served as the substrate for the working electrode, with the rotating speed varying from 100 to 1600 rpm. Ag/AgCl (3.5 M KCl) and Pt foil were used as the reference and counter electrodes in alkaline electrolyte (0.1 M KOH). The N, S-CMTs or commercial Pt/C (20 wt%, Johnson Matthey) ink was prepared by blending the electrocatalyst powder (2 mg) with 20 μL Nafion solution and 980 μL ethanol by sonication for 48 h. 20 μL N, S-CMTs ink or 10 μL commercial 20% Pt/C ink was then pipetted onto the glassy carbon surface. Electrolyte was saturated with N_2/O_2 by N_2/O_2 bubbling for 30 min prior to each experiment. The cyclic voltammetry (CV) measurements were performed in N_2- and O_2-saturated aqueous electrolyte solutions (0.1 M KOH) with a scan rate of 50 mV/s. Rotating disk electrode (RDE) measurements were conducted in O_2-saturated electrolyte with a sweep rate of 5 mV/s. In order to estimate the double layer capacitance, the electrolyte was deaerated by N_2 bubbling, then the voltammogram was evaluated in the deaerated electrolyte. The oxygen reduction current was derived as the difference between the currents measured in the deaerated and O_2-saturated electrolytes.

Electron transfer numbers were calculated using the Koutecky–Levich equation:

$$\frac{1}{j}=\frac{1}{j_{\mathrm{L}}}+\frac{1}{j_{\mathrm{K}}}=\frac{1}{B\omega^{1/2}}+\frac{1}{j_{\mathrm{K}}} \quad (1)$$

$$B=0.62nFC_0(D_0)^{2/3}v^{-1/6} \quad (2)$$

$$j_{\mathrm{K}}=nFkC_0 \quad (3)$$

where j is the measured current density, j_L and j_K are the diffusion- and kinetic-limiting current densities, respectively. n is the overall number of electrons transferred in ORR, F is the Faraday constant (F = 96485 C mol^{-1}), C_0 is the bulk concentration of O_2 (1.2×10^{-6} mol cm^{-3} in 0.1 M KOH), D_0 is the diffusion coefficient of O_2 in electrolyte (1.9×10^{-5} cm^2 s^{-1}, in 0.1 M KOH), v is the kinetic viscosity of the electrolyte (0.01 cm^2 s^{-1}, in 0.1 M KOH), ω is the angular velocity of the disk ($\omega = 2\pi N$, N is the linear rotating speed in rpm), and k is the electron transfer rate constant.

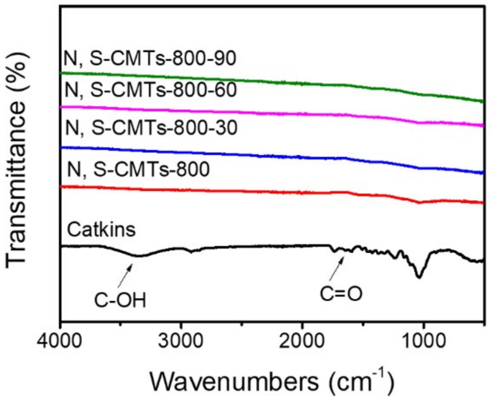

Figure S1. FTIR spectra of the catkins and N, S-CMTs-800, N, S-CMTs-800-30, N, S-CMTs-800-60, and N, S-CMTs-800-90, respectively, obtained after pyrolysis and CO_2 activation.

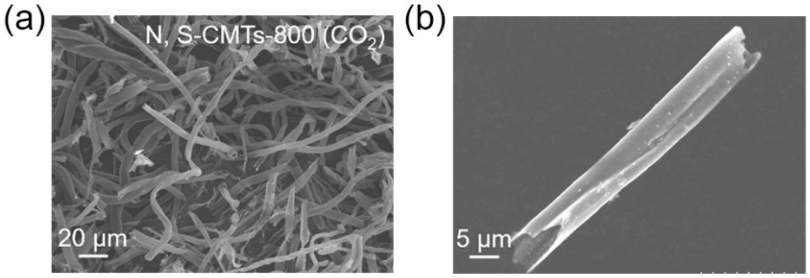

Figure S2. Low-magnification (a) and high-magnification (b) SEM images of the N, S-CMTs-800 (CO_2), prepared by CO_2 activation of the N, S-CMTs-800.

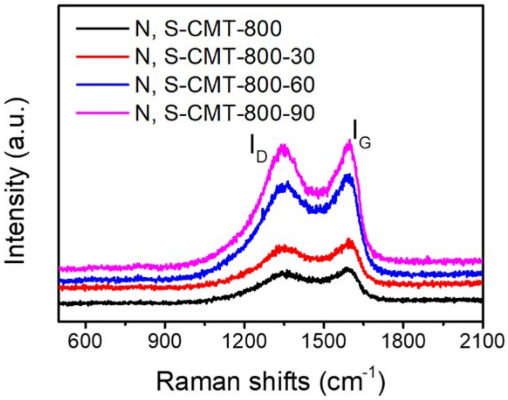

Figure S3. Raman spectra of N, S-CMTs-800, N, S-CMTs-800-30, N, S-CMTs-800-60, and N, S-CMTs-800-90.

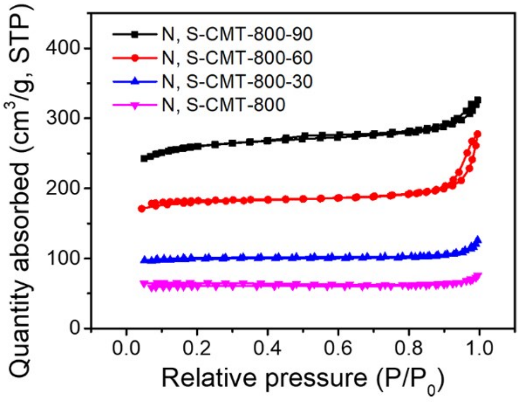

Figure S4. N_2 sorption isotherms of N, S-CMTs-800, N, S-CMTs-800-30, N, S-CMTs-800-60, and N, S-CMTs-800-90.

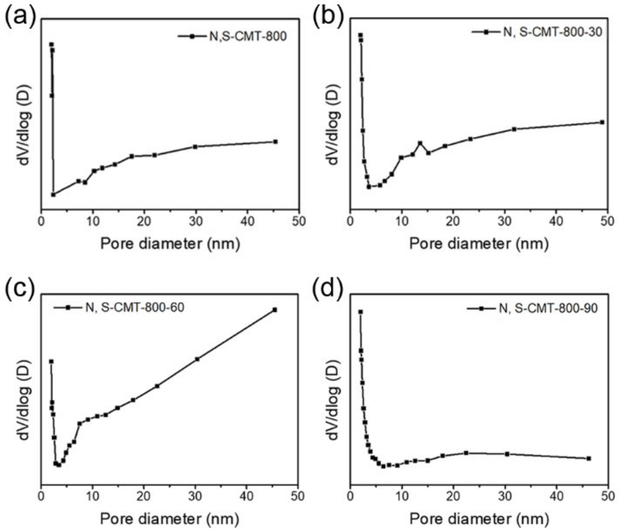

Figure S5. Pore size distribution curves of N, S-CMTs-800 (a), N, S-CMTs-800-30 (b), N, S-CMTs-800-60 (c), and N, S-CMTs-800-90 (d).

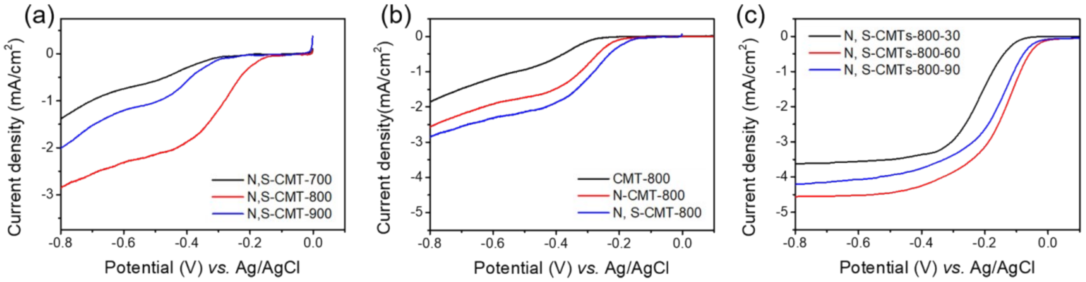

Figure S6. LSV curves of (a) N, S-CMTs-700, N, S-CMTs-800, and N, S-CMTs-900 obtained by pyrolysis of the MB/catkin hybrids at 700, 800, and 900 ^{o}C; (b) CMTs-800, N-CMTs-800, and N, S-CMTs-800 prepared with catkins, Rhodamine B/catkin hybrids, and MB/catkin hybrids at 800 ^{o}C, respectively; (c) N, S-CMTs-800-30, N, S-CMTs-800-60, and N, S-CMTs-800-90.

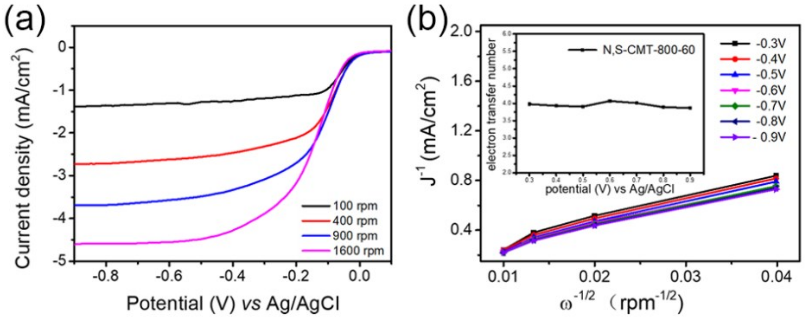

Figure S7. (a) LSV curves of N, S-CMTs-800-60 at varying rotating speeds from 100 to 1600 rpm. (b) The corresponding Koutecky-Levich plots of N, S-CMTs-800-60 from -0.9 to -0.3 V (*vs.* Ag/AgCl). The inset of (b) shows the electron transfer number as a function of the potential.

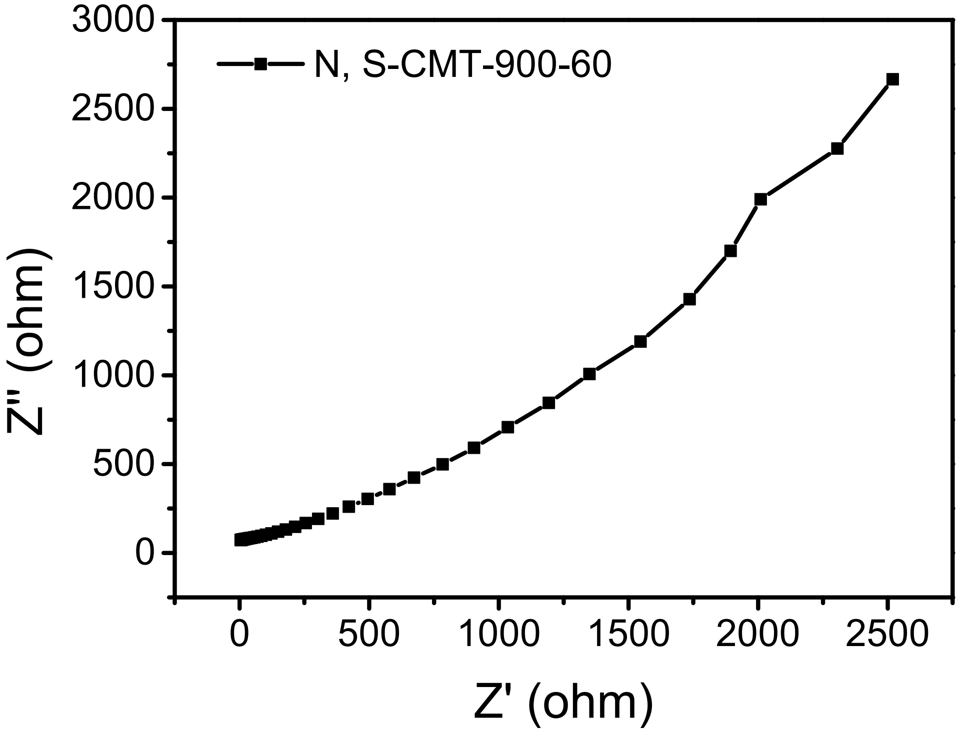

Figure S8. Nyquist plots of N, S-CNT-900-60.

Table S1. The specific surface areas and pore volumes of the samples.

	BET surface area (m^2/g)	Pore volume (cm^3/g)	Pore size (Å)
N, S-CMT-800	201.11	0.11	2.34
N, S-CMT-800-30	323.54	0.18	2.17
N, S-CMT-800-60	604.48	0.35	2.17
N, S-CMT-800-90	872.94	0.47	2.12

Table S2. XPS analysis of the surface composition of the samples.

	N, S-CNT-800	N, S-CNT-800-30	N, S-CNT-800-60	N, S-CNT-800-90
C (%)	80.31	84.39	90.77	91.71
S (%)	1.25	0.94	0.35	0.24
N (%)	1.14	0.85	0.27	0.20

Table S3. Comparison of the specific capacitances of some N-doped carbons in the literature.

	Onset potential	Half-wave potential	Limited current	Ref.
SWCNT@NPC	-	0.85 V vs. RHE	-	*Carbon* 2018, *139*, 156-163
S,S′-CNT$_{1000}$	0.87 V vs. RHE	0.79 V vs. RHE	-	*Adv. Energy Mater.* 2016, *6*, 1501966
Co/CNFs (1000)	1.01 V vs. RHE	0.896 V vs. RHE	-	*Adv. Mater.* 2019, *31*, 1808043
N/S-2DPC-60	0.86 V vs. RHE	-	-	*Adv. Funct. Mater.* 2016, *26*, 5893-5902
Fe/N-CNFs	0.88 V vs. RHE	0.79 V vs. RHE	-5.56 mA/cm^2	*small* 2016, *12,* 6398-6406
1100-CNS	-	0.88 V vs. RHE	-	*Energy Environ. Sci.* 2017, *10*, 742-749